

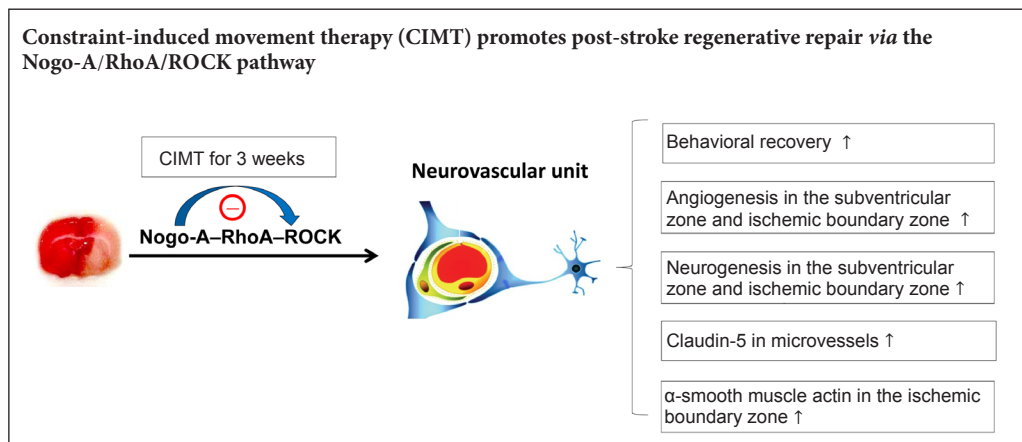
# Constraint-induced movement therapy enhances angiogenesis and neurogenesis after cerebral ischemia/reperfusion

Zhi-Yong Zhai, Juan Feng\*

Department of Neurology, Shengjing Hospital of China Medical University, Shenyang, Liaoning Province, China

**Funding:** This study was supported by the National Natural Science Foundation of China (General Program), No. 81771271 (to JF).

## Graphical Abstract



\*Correspondence to:

Juan Feng, PhD,  
juanfeng@cmu.edu.cn.

orcid:

0000-0002-1815-7036  
(Juan Feng)

doi: 10.4103/1673-5374.257528

Received: October 9, 2018

Accepted: February 11, 2019

## Abstract

Constraint-induced movement therapy after cerebral ischemia stimulates axonal growth by decreasing expression levels of Nogo-A, RhoA, and Rho-associated kinase (ROCK) in the ischemic boundary zone. However, it remains unclear if there are any associations between the Nogo-A/RhoA/ROCK pathway and angiogenesis in adult rat brains in pathological processes such as ischemic stroke. In addition, it has not yet been reported whether constraint-induced movement therapy can promote angiogenesis in stroke in adult rats by overcoming Nogo-A/RhoA/ROCK signaling. Here, a stroke model was established by middle cerebral artery occlusion and reperfusion. Seven days after stroke, the following treatments were initiated and continued for 3 weeks: forced limb use in constraint-induced movement therapy rats (constraint-induced movement therapy group), intraperitoneal infusion of fasudil (a ROCK inhibitor) in fasudil rats (fasudil group), or lateral ventricular injection of NEP1-40 (a specific antagonist of the Nogo-66 receptor) in NEP1-40 rats (NEP1-40 group). Immunohistochemistry and western blot assay results showed that, at 2 weeks after middle cerebral artery occlusion, expression levels of RhoA and ROCK were lower in the ischemic boundary zone in rats treated with NEP1-40 compared with rats treated with ischemia/reperfusion or constraint-induced movement therapy alone. However, at 4 weeks after middle cerebral artery occlusion, expression levels of RhoA and ROCK in the ischemic boundary zone were markedly decreased in the NEP1-40 and constraint-induced movement therapy groups, but there was no difference between these two groups. Compared with the ischemia/reperfusion group, modified neurological severity scores and foot fault scores were lower and time taken to locate the platform was shorter in the constraint-induced movement therapy and fasudil groups at 4 weeks after middle cerebral artery occlusion, especially in the constraint-induced movement therapy group. Immunofluorescent staining demonstrated that fasudil promoted an immune response of nerve-regeneration-related markers (BrdU in combination with CD31 (platelet endothelial cell adhesion molecule), Nestin, doublecortin, NeuN, and glial fibrillary acidic protein) in the subventricular zone and ischemic boundary zone ipsilateral to the infarct. After 3 weeks of constraint-induced movement therapy, the number of regenerated nerve cells was noticeably increased, and was accompanied by an increased immune response of tight junctions (claudin-5), a pericyte marker ( $\alpha$ -smooth muscle actin), and vascular endothelial growth factor receptor 2. Taken together, the results demonstrate that, compared with fasudil, constraint-induced movement therapy led to stronger angiogenesis and nerve regeneration ability and better nerve functional recovery at 4 weeks after cerebral ischemia/reperfusion. In addition, constraint-induced movement therapy has the same degree of inhibition of RhoA and ROCK as NEP1-40. Therefore, constraint-induced movement therapy promotes angiogenesis and neurogenesis after cerebral ischemia/reperfusion injury, at least in part by overcoming the Nogo-A/RhoA/ROCK signaling pathway. All protocols were approved by the Institutional Animal Care and Use Committee of China Medical University, China on December 9, 2015 (approval No. 2015PS326K).

**Key Words:** nerve regeneration; constraint-induced movement therapy; angiogenesis; ischemia/reperfusion; subventricular zone; Nogo-A; fasudil; neurovascular unit; tight junction protein; vascular endothelial growth factor receptor 2; neural regeneration

**Chinese Library Classification No.** R455; R364

## Introduction

Because of the limited regenerative capability of mature central neurons, there is no specific treatment to improve functional restoration after stroke (The NINDS t-PA Stroke Study Group, 1997; Ginsberg, 2008; Saver et al., 2009; Faulkner and Wright, 2018). Spontaneous axonal plasticity and functional restoration after stroke are thought to be limited by myelin-associated neurite growth inhibitory proteins in the adult central nervous system, particularly Nogo-A (Schnell, et al., 1990; Bregman, 1995; Chen et al., 2000; Gonzenbach et al., 2008; Cao et al., 2016; Lu et al., 2018). Anti-Nogo-A immunotherapy improves neurological outcomes, neuroregeneration, and neural plasticity after central nervous system lesions in adult or aged rats (Kartje et al., 1999; Liebscher et al., 2005; Tsai et al., 2011). The Rho-associated kinase (ROCK) inhibitor fasudil stimulates axonal regrowth and increases cerebral blood flow after stroke in rats (Toshima et al., 2000; Rikitake et al., 2005; Yamashita et al., 2007; Peng et al., 2018). These results suggest that reversing the Nogo-A/RhoA/ROCK pathway may contribute to recovery from ischemic brain injury. However, simply rescuing neurons after ischemic stroke is not an effective form of neuroprotection in clinical practice (Ginsberg, 2008).

Within the framework of neurovascular units, neurotransmitters are regulated and blood-brain barrier stability is maintained through cell-cell signaling between neuronal, glial, and vascular elements (Madri, 2009). Evidence suggests that both angiogenesis and neurogenesis play key roles in endogenous neuroprotection after stroke (Ruan et al., 2015). Studies have increasingly identified a close relationship and interaction between neurogenesis and angiogenesis (Palmer et al., 2000; Shen et al., 2004; Ruan et al., 2015; Lei et al., 2016). Neural and vascular cells are strongly connected, and they establish functional connectivity and crosstalk guided by similar signals (Quaegerbeur et al., 2011).

Constraint-induced movement therapy (CIMT) can promote brain repair by enhancing structural plasticity and functional reorganization after stroke (Sterling et al., 2013; Zhao et al., 2013), but the endogenous mechanisms of its regenerative effects have not been fully elucidated. In one study, Zhao et al. (2013) reported that CIMT was effective in promoting axonal regrowth in part by restraining the Nogo-A/RhoA/ROCK signaling pathway, which improved recovery after cerebral ischemia in rats. The myelin-associated neurite growth inhibitor Nogo-A is a negative regulator of angiogenesis in the early postnatal brain, and the effect of Nogo-A on microvascular endothelial cells requires the intracellular activation of the RhoA/ROCK-Myosin II pathway (Wälchli et al., 2013). In one study, adult Nogo-A<sup>-/-</sup> mice had no significant changes in blood vessel densities in any of the examined brain areas. It is unclear whether there are any associations between Nogo-A/RhoA/ROCK and angiogenesis in adult rats during pathological processes such as stroke. In addition, it has not yet been reported whether CIMT can promote angiogenesis in stroke in adult rats by overcoming Nogo-A/RhoA/ROCK signaling.

Newborn microvessels can promote the proliferation of

endogenous nerve precursor cells in the subventricular and subgranular zones, as well as their migration to the infarct area and further differentiation into mature neurons and glial cells (Taguchi et al., 2004). From the perspective of protecting neurovascular units, we examined the effects of CIMT on angiogenesis, endogenous neurogenesis, and behavioral recovery in rats after stroke. We also clarified whether the inhibitory effect of CIMT on the Nogo-A/RhoA/ROCK pathway was enough to induce its regenerative effects.

## Materials and Methods

### Animals and treatment

Seventy-two male specific-pathogen-free Sprague-Dawley rats aged 8–10 weeks old and weighing 280–320 g were provided by Beijing Huafukang Biotechnology Co., Ltd., China [License No. SCXK (Jing) 2014-0004]. All protocols were approved by the Institutional Animal Care and Use Committee of China Medical University, China on December 9, 2015 (approval No. 2015PS326K). All experimental procedures described here were in accordance with the National Institutes of Health (NIH) guidelines for the Care and Use of Laboratory Animals (Publication No. 85-23, revised 1996). Animals were sacrificed using an overdose of sodium pentobarbital, and all efforts were made to minimize animal suffering.

The experiment included two parts, as follows:

(1) An experiment examining the effects of fasudil and CIMT was conducted in 36 adult rats; the rats survived for 4 weeks after middle cerebral artery occlusion (MCAO). Before surgery, the rats were randomly assigned to Sham1 (no MCAO, vehicle;  $n = 6$ ), IR1 (MCAO + vehicle;  $n = 10$ ), fasudil (MCAO + fasudil;  $n = 10$ ), or CIMT1 (MCAO + CIMT;  $n = 10$ ) groups. In this experiment, 18 rats were used for immunohistochemistry and 18 rats were used for western blot assay (for each, Sham1:  $n = 3$  and all other groups:  $n = 5$ ).

(2) A second experiment was conducted to determine the extent of the impact of CIMT and NEP1-40 (a specific antagonist of the Nogo-66 receptor) treatment on the Nogo-A/RhoA/ROCK pathway. In this experiment, 36 rats were randomly divided into two groups (the 2-week or 4-week group) and sacrificed at 2 weeks or 4 weeks after stroke. Eighteen rats were used at each time point. The rats in each group were randomly assigned to the following treatment and control groups: Sham2 (no MCAO, vehicle;  $n = 3$ ), IR2 (MCAO + vehicle;  $n = 5$ ), NEP1-40 [MCAO + NEP1-40;  $n = 5$ ], and CIMT2 (MCAO + CIMT;  $n = 5$ ).

The rats were housed at a controlled temperature with a 12-hour light/dark cycle. They had free access to food and water and were food-deprived for 12 hours before surgery.

### Induction of focal cerebral ischemia/reperfusion injury

Right MCAO was induced to create a focal ischemia/reperfusion injury in adult male rats, as previously described (Longa et al., 1989). Briefly, rats were anesthetized with 5% isoflurane and maintained with 2% isoflurane in an oxygen/

air mixture. The right common carotid artery was exposed and a nylon suture (0.26 mm diameter) coated with polylysine was inserted into the right internal carotid artery, through the external carotid artery, and advanced until it occluded the origin of the middle cerebral artery. The intraluminal filament was carefully withdrawn to establish reperfusion after 90 minutes of MCAO. The completeness of occlusion and reperfusion were confirmed by laser Doppler (Pari Medical Technology (Beijing) Co., Ltd., Beijing, China). At least a 70% reduction in blood flow values relative to baseline in the middle cerebral artery area was needed to confirm occlusion by laser Doppler. Sham-operated rats underwent similar surgical procedures without occlusion of the MCA. Body temperature was maintained at  $37 \pm 0.5^\circ\text{C}$  with a thermoregulated heating pad throughout the surgery.

### Cannula implant

A cannula implant was inserted 1 week after ischemia/reperfusion and lasted for 1 or 3 weeks. Anesthesia was induced using 5% isoflurane and maintained with 2% isoflurane, and rats were fixed in a stereotaxic apparatus (Biowill Co., Ltd., Shanghai, China) during surgery. A hole was drilled into the skull of the damaged hemisphere according to the following coordinates in relation to bregma (Paxinos et al., 2005): anteroposterior  $-0.9$  mm and mediolateral  $+2.0$  mm. A cannula (Alzet Brain Infusion Kit II; Alzet Scientific Products, Cupertino, CA, USA) connected to a catheter was implanted into the lateral ventricle at a depth of 4.0 mm from the pial surface (Lee et al., 2004). The other end of the catheter was sealed under the skin. Either vehicle or drug was continuously infused into the lateral ventricle *via* osmotic minipumps (Alzet model 2ML4, Alzet Scientific Products).

### CIMT treatment

Seven days after ischemia/reperfusion, CIMT was achieved by fitting each rat in the CIMT group with a one-sleeve plaster cast. The plaster was applied to restrain the unaffected upper limb and to force the dominant use of the affected limb in daily activities (Taub et al., 2006). Soft cotton pads were used in the plaster to allow moderate, but not excessive, movements of the upper limb (Ishida et al., 2015). CIMT plaster casts were not removed until behavioral tests were conducted or rats were sacrificed. Rats were forced to use their affected forelimb on a motorized treadmill (SANS Biological Technology Co., Ltd., Jiangsu, China) set at a speed of 5 m/min. CIMT was conducted for 10 minutes every day, 4 days per week, for 3 weeks.

### Drug treatment

In the first experiment, fasudil (Selleck, Houston, USA; ROCK inhibitor) was dissolved in sterile distilled water to a final concentration of 2.5 mg/mL. For rats in the fasudil group, fasudil was intraperitoneally injected once daily at a dose of 10 mg/kg, starting 1 week after MCAO and lasting for 3 weeks. Rats in the other groups received intraperitoneal injections of 0.9% saline solution.

In the second experiment, at 7 days after MCAO, rats were anesthetized with 10% chloral hydrate and the skin over the

back was incised. The catheter was connected to an osmotic minipump filled with either 1 mg NEP1-40 (Sigma-Aldrich, St. Louis, MO, USA) in 2 mL vehicle (group NEP1-40) or 2 mL vehicle (97.5% phosphate-buffered saline + 2.5% dimethyl sulfoxide; CIMT2, IR2, and Sham2 groups) (Lee et al., 2004). The pump continuously delivered the solution at 2.5  $\mu\text{L}/\text{hour}$  for 1 or 3 weeks.

### 5-Bromo-2-deoxyuridine (BrdU) labeling

From 7 days after MCAO-reperfusion or sham surgery, BrdU (Sigma-Aldrich) was intraperitoneally administered every second day for 3 weeks to investigate cell renewal processes. BrdU was injected at a dose of 50 mg/kg.

### Behavioral tests

Modified neurological severity scores (mNSS) were performed at 1 day and 4 weeks after MCAO and reperfusion. Rats were tested for beam walking and water maze performance at 4 weeks after MCAO and reperfusion. A 3-day pre-training was performed before formal tests of beam walking and water maze. The mNSS was used to assess basic motor ability of rats, as described in a previous study (Hunter et al., 2000). The mNSS ranged from 0 to 18, and included tests of motor, sensory, reflex, and balance performance. Sensorimotor function of the impaired limbs was evaluated by a tapered/ledged-beam-walking test (Zhao et al., 2005). The walking process was video recorded and analyzed by calculating the foot fault score according to the following formula:

Foot fault score = number of slips/number of total steps.

Spatial learning was measured in a Morris water maze as previously described (Hosseini-Sharifabad et al., 2011). Live video was recorded to evaluate escape latency (time taken to locate the platform). Each rat was scored by two investigators in a blinded fashion.

### Immunofluorescence and immunohistochemistry

Briefly, brains were fixed by transcardial perfusion and immersion in 4% paraformaldehyde. Brain tissue was prepared, paraffin sectioned, and cut into 20  $\mu\text{m}$  coronal slices. Sections were dewaxed and rehydrated, and then put into antigen repair solution and continuously heated for 10 minutes over low heat for antigen retrieval. Sections were then incubated in 3%  $\text{H}_2\text{O}_2$  solution for 15 minutes at room temperature to inactivate endogenous peroxidase activity. After blocking with normal goat serum for 15 minutes, sections were incubated at  $4^\circ\text{C}$  overnight in the following primary antibodies: rabbit anti-Nogo-A (polyclonal, 1:50; Abcam, Cambridge, UK), rabbit anti-RhoA (polyclonal, 1:200; Abcam), rabbit anti-ROCK (monoclonal, 1:100; Abcam), mouse anti-BrdU (monoclonal, 1:500; Sigma-Aldrich), rabbit anti-platelet endothelial cell adhesion molecule (CD31; polyclonal, 1:100; Abcam), rabbit anti-claudin-5 (polyclonal, 1:150; Abcam), rabbit anti- $\alpha$ -smooth muscle actin ( $\alpha$ -SMA; polyclonal, 1:100; Abcam) and rabbit anti-vascular endothelial growth factor receptor 2 (VEGFR2; polyclonal, 1:100; Abcam). Sections were then incubated with biotin-labeled goat anti-rabbit IgG (1:200; Beyotime, Shanghai, China) at  $37^\circ\text{C}$  for 30 minutes before being incubated in horse-

radish-peroxidase-labeled streptavidin working fluid at 37°C for 30 minutes. Negative controls were established by replacing the primary antibody with phosphate-buffered saline. A diaminobenzidine chromogenic method was used. To study angiogenic- and neurogenic-related events, some sections were double incubated at 4°C overnight with BrdU/CD31 (polyclonal, 1:100; Abcam), BrdU/nestin (polyclonal, 1:500; Proteintech, Chicago, IL, USA), BrdU/doublecortin (DCX; polyclonal, 1:800; Abcam), BrdU/NeuN (monoclonal, 1:500; Abcam) or BrdU/glia fibrillary acidic protein (GFAP; polyclonal, 1:1000; Abcam) as surrogate markers of neurogenesis. Secondary antibodies included fluorescein isothiocyanate (FITC)-labeled goat anti-rabbit IgG and Cy3-labeled goat anti-mouse IgG (1:300; Beyotime), and sections were incubated for 90 minutes at room temperature. Nuclei were counterstained with 4',6-diamidino-2-phenylindole (DAPI; 1:1000; Sigma-Aldrich) in the dark at 37°C for 10 minutes. DAPI-labeled nuclei were blue, FITC-labeled proliferating cells were green, and BrdU-positive cells were labeled red by Cy3. Pictures were merged, and the positive BrdU/proliferating cells were determined. Image-Pro Plus version 6.0 software (Media Cybernetics, Rockville, MD, USA) was used to quantitatively analyze positive cells.

To determine cellular proliferation in the subventricular zone, every tenth section between bregma levels +1.0 mm and -0.3 mm was selected (five sections per brain). Immunofluorescence images of BrdU<sup>+</sup>/CD31<sup>+</sup>, BrdU<sup>+</sup>/nestin<sup>+</sup>, and BrdU<sup>+</sup>/DCX<sup>+</sup> cells were acquired at 200× magnification in the subventricular zone, ipsilateral to the infarct. Immunopositive cells were counted in five sections and a mean cell count per section was obtained. Immunofluorescence images of neurogenic markers in the ischemic boundary zone (BrdU<sup>+</sup>/NeuN<sup>+</sup> or BrdU<sup>+</sup>/GFAP<sup>+</sup>) of every tenth section between bregma levels +1.7 mm and +0.7 mm were captured at 400× magnification. Cells in the peri-infarct cortex that were immunopositive for CD31 (newborn microvessels),  $\alpha$ -SMA (pericytes), Nogo-A, RhoA, ROCK (pathway proteins), and VEGFR2 were counted from immunohistochemistry images taken with a 400× objective (every tenth section between bregma levels +3.2 mm and -0.3 mm were counted; five sections per brain). Immunopositivity for claudin-5 was quantified by mean optical density using Image-Pro Plus version 6.0 software (Media Cybernetics). All experimental procedures were conducted by two investigators in a double-blinded fashion.

### Western blot assays

Briefly, protein samples were extracted from the peri-infarct cortex. Equal amounts of protein samples were subjected to 10% sodium dodecyl sulfate-polyacrylamide gel electrophoresis and electrophoretically transferred onto polyvinylidene fluoride membranes. Immunoblotting was performed with rabbit primary antibodies corresponding to CD31 (polyclonal, 1:800; Abcam), claudin-5 (polyclonal, 1:1000; Abcam), VEGFR2 (polyclonal, 1:1000; Abcam) and  $\beta$ -actin (polyclonal, 1:1000; Wanleibio, Shenyang, China) at 4°C overnight. Peroxidase-conjugated secondary antibodies

(goat anti-rabbit, 1:5000; Wanleibio) were then used.  $\beta$ -Actin served as the internal loading control. Integrated density values of bands were measured using Quantity One Software (Bio-Rad, Hercules, CA, USA). The optical density value ratio of the target band to the internal reference was used for quantification of each protein.

### Statistical analysis

Data were compiled and analyzed using SAS 9.1 software (SAS Institute Inc., Cary, NC, USA). All data are expressed as the mean  $\pm$  SD. Significant differences among groups were determined by one-way analysis of variance followed by Student-Newman-Keuls *post hoc* analysis. A *P*-value of less than 0.05 was considered statistically significant.

## Results

### Quantitative analysis of animals

A total of 82 rats were used in this study. Six rats died after MCAO surgery, and four died after cannula implant. All sham-operated rats survived. During model establishment, the dead rats were randomly supplemented by new rats to ensure there were sufficient numbers of animals in each group.

### CIMT stimulates angiogenesis in the subventricular zone and ischemic boundary zone

Rats were treated with either fasudil or CIMT from 7 days after ischemia/reperfusion to investigate the role of CIMT in angiogenesis. The treatment effects were then measured at 4 weeks post-stroke. During an angiogenesis assay, we observed cells labeled with CD31, a marker for newly formed microvessels, in the subventricular zone using BrdU/CD31 immunofluorescence and in the ischemic boundary zone using immunohistochemical staining. Quantitative determination of BrdU/CD31-positive vasculature in the subventricular zone suggested that, compared with the IRI group, vascular density was enhanced in the CIMT1 and fasudil groups. Moreover, CIMT-treated rats had more BrdU/CD31-positive vessels in the subventricular zone compared with fasudil-treated rats ( $P < 0.05$ ) (Figure 1A and B). Western blots confirmed a robust upregulation of CD31 expression after both CIMT and fasudil treatment (Figure 1C and D). The ischemic boundary zone exhibited similar outcomes (Figure 2).

### CIMT improves behavioral recovery

To test whether angiogenesis in the subventricular zone and ischemic boundary zone was associated with improved behavioral outcomes in ischemic rats, behavioral assessments were conducted at 1 day and 4 weeks after MCAO. All rats showed similar mNSS scores, and there were no differences among the groups at 1 day after MCAO ( $P > 0.05$ ; Figure 3A). However, all rats showed improvement in behavioral outcomes over time (Figure 3A). At 4 weeks after MCAO, there was a significant difference in foot fault scores in the tapered-beam-walking test among the groups ( $F = 63.93$ ,  $P < 0.0001$ ). Foot faults for the impaired forelimbs of fasudil-treated rats were significantly lower than those of IRI

rats ( $P < 0.01$ ). Furthermore, the CIMT1 group had lower foot fault scores than both the fasudil and IR1 groups ( $P < 0.01$ ; **Figure 3B**).

In the water maze test, there were also significant group effects in escape latency ( $F = 32.69$ ,  $P < 0.0001$ ). The time to locate the platform was shorter in the CIMT1 and fasudil groups than in the IR1 group. In addition, escape latency was shorter in the CIMT1 group than in the fasudil group ( $P < 0.05$ , **Figure 3C**). These results demonstrated that CIMT treatment improved cognitive outcomes in rats after stroke.

#### **CIMT stimulates cell proliferation in the subventricular zone**

Enhanced neurogenesis and angiogenesis play an important role in neuronal self-repair after cerebral ischemia (Ruan et al., 2015). A growing number of studies have identified a close interactive relationship between neurogenesis and angiogenesis (Palmer et al., 2000; Shen et al., 2004; Ruan et al., 2015; Lei et al., 2016). We examined the proliferation of endogenous neural stem cells using BrdU/nestin immunofluorescence at 4 weeks after stroke. Quantitative analysis indicated that BrdU/nestin expression levels in the subventricular zone were markedly elevated in the CIMT1 and fasudil groups compared with the IR1 group. Moreover, compared with fasudil treatment, CIMT treatment significantly increased the number of BrdU/nestin-positive cells (**Figure 4**). In addition, we investigated subventricular zone expression of DCX, which is expressed by neuronal precursor cells and immature neurons, using BrdU and DCX double staining at 4 weeks after stroke. Cerebral ischemia upregulated BrdU/DCX-positive cell numbers, and compared with fasudil and IR treatment, CIMT treatment further increased the number of BrdU/DCX-positive cells (**Figure 5**).

#### **CIMT stimulates neurogenesis in the ischemic boundary zone**

Markers of neurogenesis were also analyzed in the ischemic boundary zone at 4 weeks after stroke. BrdU expression was enhanced in the peri-infarct regions. As expected, the ischemic boundary zone showed an increase in neurogenic markers, and fasudil treatment further increased the number of BrdU/NeuN-positive cells (new adult neurons) in the cortex ipsilateral to the infarct. The number of BrdU/NeuN-positive cells was markedly increased after 3 weeks of CIMT treatment compared with the same period of fasudil treatment (**Figure 6**). A similar result was observed for BrdU/GFAP-positive cells, indicating gliogenesis, in the ischemic boundary zone, but there was no significant difference between the fasudil and CIMT1 groups for these markers (**Figure 7**).

#### **CIMT increases claudin-5 expression in cerebral microvessels**

Communication between the central nervous system and microvessels, known as the blood-brain barrier, is mediated through the neurovascular unit, which comprises endothelial cells, pericytes, astrocytes, neurons, and perivascular

macrophages. The blood-brain barrier, with its unique properties, maintains central nervous system homeostasis. At 4 weeks after MCAO, the tight junction marker claudin-5 was investigated to characterize the barrier properties of the blood-brain barrier. Cerebral ischemia noticeably decreased the mean optical density values of claudin-5, while fasudil and CIMT treatment visibly increased the mean optical density values of claudin-5. However, claudin-5 expression was much higher in the CIMT1 group than in the fasudil group (**Figure 8A and B**). Western blot assays also gave similar results (**Figure 8C and D**). The results suggest that CIMT may be an effective treatment to improve blood-brain barrier integrity after damage by cerebral ischemia.

#### **CIMT increases $\alpha$ -SMA expression in the ischemic boundary zone**

Central nervous system endothelial cells and perivascular support cells, including pericytes and perivascular astrocytes, are involved in blood-brain barrier formation, maintenance, and stability (Daneman et al., 2010; Quaegebeur et al., 2011; Hill et al., 2014). For this reason,  $\alpha$ -SMA, a pericyte marker, was investigated in the ischemic boundary zone using immunohistochemistry (**Figure 9A**). Treatment with fasudil and CIMT increased the number of  $\alpha$ -SMA-positive vessels compared with the IR1 group. Moreover, CIMT-treated rats had more  $\alpha$ -SMA-positive vessels in the ischemic boundary zone than did fasudil-treated rats ( $P < 0.05$ ; **Figure 9B**).

#### **CIMT promotes post-stroke angiogenesis and neurogenesis in part by overcoming the Nogo-A/RhoA/ROCK pathway**

The Nogo-A/RhoA/ROCK pathway is necessary for functional recovery after stroke, and its expression may be affected by CIMT (Zhao et al., 2013). In a previous study, application of the neutralizing antibody, fasudil, induced regenerative repair after stroke. Thus, to determine whether CIMT influenced the Nogo-A/RhoA/ROCK pathway in its induction of angiogenesis and neurogenesis, we used NEP1-40, an inhibitor of the Nogo-A receptor. Expression levels of Nogo-A, RhoA, and ROCK were notably increased in the ischemic boundary zone compared with in the Sham2 cortex. Nogo-A expression was not affected by NEP1-40, while expression levels of RhoA and ROCK were significantly decreased by NEP1-40 ( $P < 0.05$ ). At 2 weeks after MCAO, expression levels of RhoA and ROCK were lower in rats treated with NEP1-40 than in rats treated with CIMT (**Figure 10**). However, at 4 weeks after MCAO, expression levels of RhoA and ROCK were decreased in the NEP1-40 and CIMT2 groups, but there was no clear difference between these two groups (**Figure 11**). These results demonstrate that CIMT promoted post-stroke angiogenesis and neurogenesis at least partly by overcoming Nogo-A-RhoA-ROCK signaling, with a time-dependent mechanism.

#### **CIMT induces VEGFR2 expression**

The aforementioned results indicate that the Nogo-A/RhoA/ROCK pathway plays a central role in CIMT-medi-

ated injury reduction in the neurovascular unit after stroke. Furthermore, compared with the fasudil group, angiogenesis, neurogenesis, and functional recovery were markedly increased in the CIMT1 group, which suggests that other potential mechanisms also participate in CIMT-induced

neuroprotection. VEGFR2 is an important regulator in the signal transduction of VEGF-A-mediated central nervous system angiogenesis (Mancuso et al., 2008). To investigate whether VEGF-A/VEGFR2 expression was affected by CIMT, we compared VEGFR2 expression levels in brains of rats treated with CIMT and fasudil at 4 weeks after MCAO.

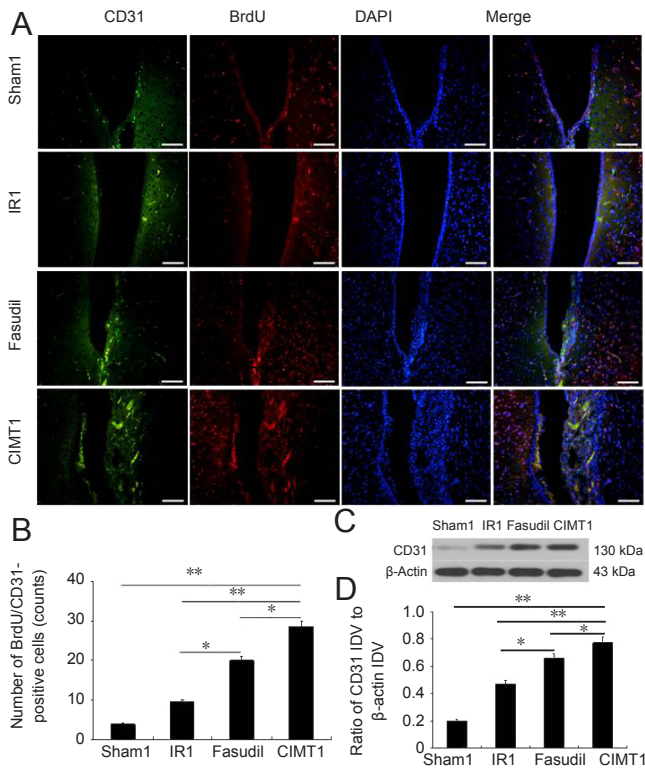


**Figure 1** CIMT enhances angiogenesis in the subventricular zone after middle cerebral artery occlusion. (A) Double immunofluorescence images of BrdU/CD31-positive cells in the Sham1 (no MCAO, vehicle), IR1 (MCAO + vehicle), fasudil (MCAO + a ROCK inhibitor fasudil), and CIMT1 (MCAO + CIMT) groups 4 weeks after stroke. Nuclei were labeled blue by DAPI, CD-31-positive cells were labeled green by FITC, and BrdU-positive cells were labeled red by Cy3. Scale bars: 100  $\mu$ m. (B) Quantitative determination of mean BrdU/CD31-positive cell numbers in each group. BrdU/CD31-positive cells were quantified by counting at a 200 $\times$  microscopic field of view. (C) Representative protein expression bands of CD31 measured by western blot assay 4 weeks after middle cerebral artery occlusion. (D) The ratio of CD31 IDV to  $\beta$ -actin IDV 4 weeks after middle cerebral artery occlusion. (B, D) Data are expressed as the mean  $\pm$  SD ( $n = 5$ ; one-way analysis of variance followed by the Student-Newman-Keuls *post hoc* analysis). \* $P < 0.05$ , \*\* $P < 0.01$ . CIMT: Constraint-induced movement therapy; BrdU: 5-Bromo-2-deoxyuridine; IR: ischemia/reperfusion; DAPI: 4',6-diamidino-2-phenylindole; IDV: integrated density value; MCAO: middle cerebral artery occlusion.

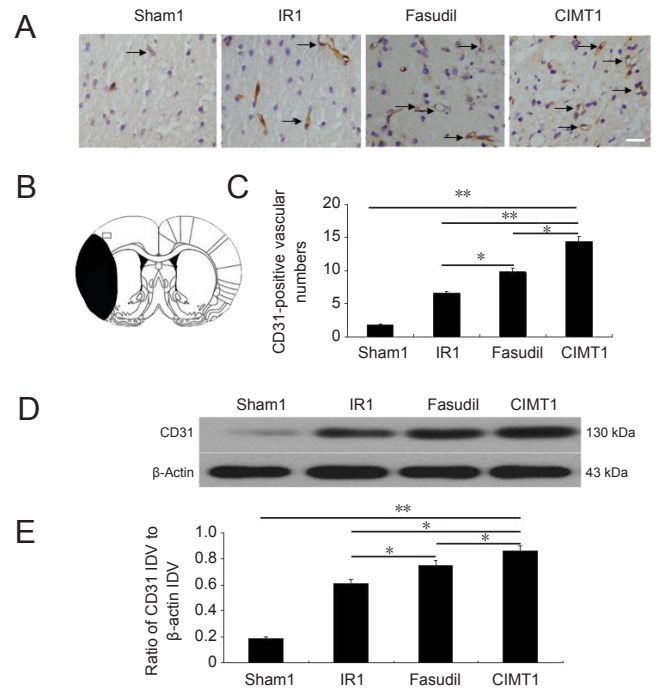


**Figure 2** CIMT enhances angiogenesis in the ischemic boundary zone after middle cerebral artery occlusion. (A) Immunohistochemistry images of CD31-positive vessels in the Sham1 (no MCAO, vehicle), IR1 (MCAO + vehicle), fasudil (MCAO + a ROCK inhibitor fasudil), and CIMT1 (MCAO + CIMT) groups at 4 weeks after stroke. Black arrows indicate CD31-positive vessels. Scale bar: 40  $\mu$ m. (B) Representative section drawing for the ischemic boundary zone, showing the region that was sampled for CD31-vessel histology in the micrographs (box). This drawing also applies to all other immunohistochemical images from the ischemic boundary zone. (C) Quantitative determination of mean CD31-positive vessel numbers in each group at 4 weeks after middle cerebral artery occlusion. (D) Representative protein expression bands of CD31 measured by western blot assay 4 weeks after middle cerebral artery occlusion. (E) The ratio of CD31 IDV to  $\beta$ -actin IDV at 4 weeks after middle cerebral artery occlusion. (B, D) Data are expressed as the mean  $\pm$  SD ( $n = 5$ ; one-way analysis of variance followed by the Student-Newman-Keuls *post hoc* analysis). \* $P < 0.05$ , \*\* $P < 0.01$ . CIMT: Constraint-induced movement therapy; IR: ischemia/reperfusion; IDV: integrated density value; MCAO: middle cerebral artery occlusion.

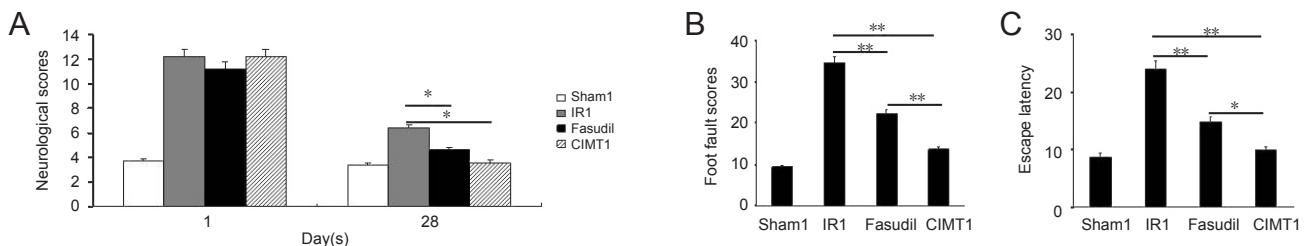


**Figure 3** CIMT improves behavioral recovery after stroke in rats after middle cerebral artery occlusion. (A) Basic motor deficits evaluated using mNSS at 1 day and at 4 weeks after middle cerebral artery occlusion. A higher mNSS score indicates a more serious basic motor deficit. (B) Foot fault scores in the tapered-beam-walking test. (C) Escape latency in the Morris water maze test. Data are expressed as the mean  $\pm$  SD ( $n = 5$ ; one-way analysis of variance followed by the Student/Newman/Keuls *post hoc* analysis). \* $P < 0.05$ , \*\* $P < 0.01$ . CIMT: Constraint-induced movement therapy; mNSS: modified neurological severity scores; MCAO: middle cerebral artery occlusion. Sham1: No MCAO, vehicle; IR1: MCAO + vehicle; fasudil: MCAO + a ROCK inhibitor fasudil; CIMT1: MCAO + CIMT.

VEGFR2 expression was increased in the ischemic boundary zone of the impaired cortex after stroke. The numbers of VEGFR2-positive cells did not change significantly in rats treated with fasudil. In contrast, there was a significant increase in VEGFR2-positive cells in the CIMT1 group ( $P$

$< 0.05$ ; **Figure 12A and B**), which was further confirmed by western blot assays (**Figure 12C and D**). These data indicate that CIMT has a positive regulatory effect on angiogenesis and neurogenesis *in vivo* through a pathway besides the No-go-A-RhoA-ROCK pathway.

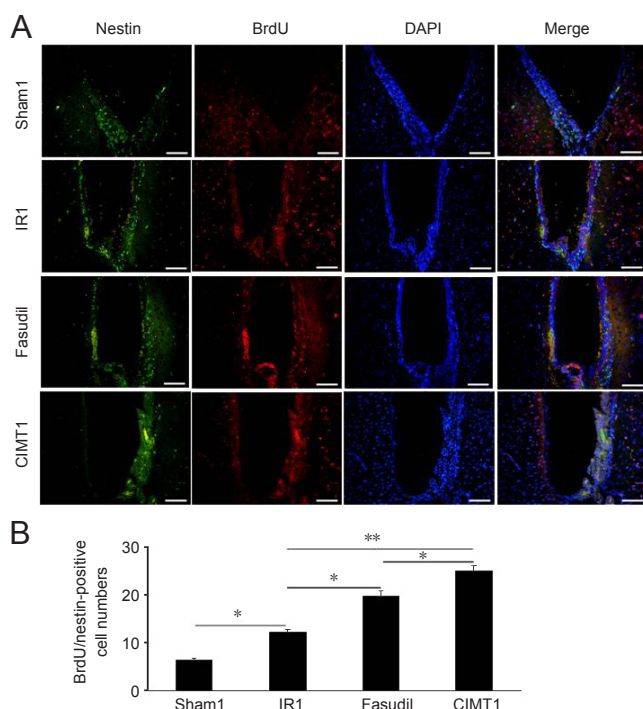


**Figure 4** Effects of CIMT on the proliferation of endogenous neural stem cells in the subventricular zone.

(A) Double immunofluorescence images of BrdU/nestin-positive cells in the Sham1 (no MCAO, vehicle), IR1 (MCAO + vehicle), fasudil (MCAO + a ROCK inhibitor fasudil), and CIMT1 (MCAO + CIMT) groups at 4 weeks after stroke. Nuclei were labeled blue by DAPI, nestin-positive cells were labeled green by FITC, and BrdU-positive cells were labeled red by Cy3. Scale bars: 100  $\mu$ m. (B) Quantitative determination of mean BrdU/nestin-positive cell numbers. BrdU/nestin-positive cells were quantified by counting at a 200 $\times$  microscopic field of view. Data are expressed as the mean  $\pm$  SD ( $n = 5$ ; one-way analysis of variance followed by the Student-Newman-Keuls *post hoc* analysis). \* $P < 0.05$ , \*\* $P < 0.01$ . CIMT: Constraint-induced movement therapy; BrdU: 5-bromo-2-deoxyuridine; IR: ischemia/reperfusion; DAPI: 4',6-diamidino-2-phenylindole; MCAO: middle cerebral artery occlusion.

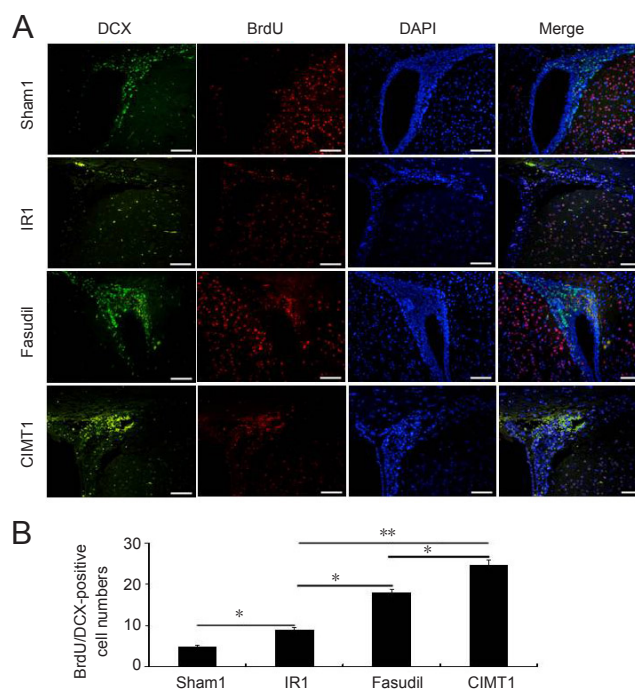


**Figure 5** Effects of CIMT on the proliferation of neural precursor cells in the subventricular zone.

(A) Double immunofluorescence images of BrdU/DCX-positive cells in the Sham1 (no MCAO, vehicle), IR1 (MCAO + vehicle), fasudil (MCAO + a ROCK inhibitor fasudil), and CIMT1 (MCAO + CIMT) groups at 4 weeks after stroke. Nuclei were labeled blue by DAPI, DCX-positive cells were labeled green by FITC, and BrdU-positive cells were labeled red by Cy3. Scale bars: 100  $\mu$ m. (B) Quantitative determination of mean BrdU/DCX-positive cell numbers. BrdU/DCX-positive cells were quantified by counting at a 200 $\times$  microscopic field of view. Data are expressed as the mean  $\pm$  SD ( $n = 5$ ; one-way analysis of variance followed by the Student-Newman-Keuls *post hoc* analysis). \* $P < 0.05$ , \*\* $P < 0.01$ . CIMT: Constraint-induced movement therapy; BrdU: 5-bromo-2-deoxyuridine; DCX: doublecortin; IR: ischemia/reperfusion; DAPI: 4',6-diamidino-2-phenylindole; MCAO: middle cerebral artery occlusion.

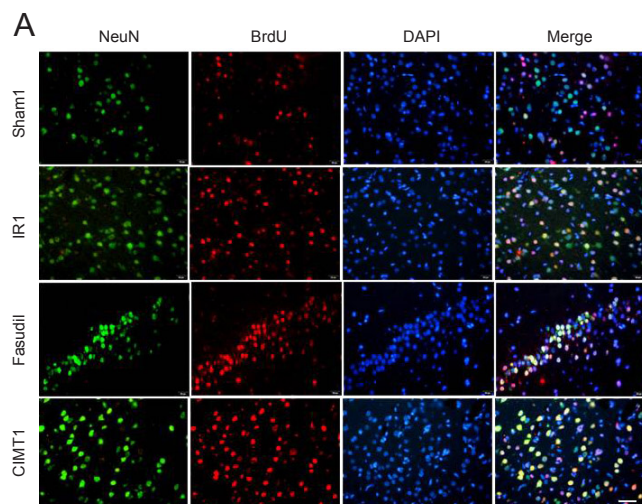


**Figure 6** CIMT increases the number of new adult neurons in the ischemic boundary zone.

(A) Double immunofluorescence images of BrdU/NeuN-positive cells in the Sham1 (no MCAO, vehicle), IR1 (MCAO + vehicle), fasudil (MCAO + a ROCK inhibitor fasudil), and CIMT1 (MCAO + CIMT) groups at 4 weeks after stroke. Nuclei were labeled blue by DAPI, NeuN-positive cells were labeled green by FITC, and BrdU-positive cells were labeled red by Cy3. Scale bar: 100  $\mu$ m. (B) Quantitative determination of mean BrdU/NeuN-positive cell numbers. BrdU/NeuN-positive cells were quantified by counting at a 400 $\times$  microscopic field of view. Data are expressed as the mean  $\pm$  SD ( $n = 5$ ; one-way analysis of variance followed by the Student-Newman-Keuls *post hoc* analysis). \* $P < 0.05$ , \*\* $P < 0.01$ . CIMT: Constraint-induced movement therapy; BrdU: 5-bromo-2-deoxyuridine; NeuN: neuron-specific nuclear protein; IR: ischemia/reperfusion; DAPI: 4',6-diamidino-2-phenylindole; MCAO: middle cerebral artery occlusion.

## Discussion

The present study demonstrated that CIMT increased both angiogenesis and neurogenesis in rats after stroke, thereby improving behavioral outcomes. In addition, by 4 weeks after ischemia, CIMT treatment decreased the expression levels of Nogo-A/RhoA/ROCK in the ischemic boundary zone to the same extent as NEP1-40. We also found that CIMT exerted further beneficial effects, promoting angiogenesis followed by endogenous neurogenesis and blood-brain barrier repair, and was superior to fasudil treatment in rats following stroke. Our results suggest that, at least in part, CIMT promoted regenerative repair through the downregulation of Nogo-A/RhoA/ROCK expression levels, and that there may be other mechanisms involved, such as the upregulation of VEGFR2 expression. We propose that CIMT may be a promising strategy for protecting the neurovascular unit after focal cerebral ischemia.

Because of the short therapeutic window for intravenous thrombolysis and endovascular interventions, very few patients receive effective treatment. CIMT is considered an attractive restorative therapy that involves the restraint of an intact upper limb (Taub et al., 2006). The main advantage of CIMT is its extended therapeutic time window, which enables more patients to benefit from this restorative therapy, such as chronic stroke patients (Gertz et al., 2006; Ueno et al., 2012). CIMT can promote brain repair by enhancing structural plasticity and functional reorganization after stroke (Sterling et al., 2013; Zhao et al., 2013), although the endogenous mechanisms of its regenerative effects have not been fully elucidated. However, growing numbers of studies have revealed some of the mechanisms underlying brain plasticity, including axonal and dendritic reorganization, angiogenesis, and neurogenesis (Gertz et al., 2006; Hermann et al., 2012; Ueno et al., 2012). Angiogenesis is an essential part of the regeneration process in ischemic tissue. However, the extent of spontaneous neovascularization that occurs after stroke cannot meet the amount needed for rehabilitation. Recent studies suggest that rehabilitation has beneficial effects on endothelial cells, including on platelet activation, cell adhesion, and cell protection (Marsh et al., 2005). In the present study, CD31 was used as a marker for newborn microvessels. At 4 weeks after MCAO, the density of microvessels in both the ischemic boundary zone and subventricular zone was observed to be increased after CIMT treatment compared with ischemia/reperfusion. Nogo-A is a negative regulator of angiogenesis in the early postnatal brain, and requires the intracellular activation of the RhoA/ROCK-Myosin II pathway. In a previous study, adult Nogo-A<sup>-/-</sup> mice had no significant changes in blood vessel densities in any of the examined brain areas (Wälchli et al., 2013). Our results suggest that fasudil can promote angiogenesis in adult rats via the inhibition of Nogo-A in pathological processes such as stroke. This is probably because Nogo-A is rapidly reduced in neurons after birth, and mainly exists on the surface of oligodendrocytes in the mature central nervous system. Nogo-A expression increases due to the repair of nerve and connective tissue after cerebral tissue ischemia and

necrosis, and fasudil can play a role in this process by inhibiting Nogo-A (Huber et al., 2002). We found that CIMT promoted angiogenesis in adult rats after stroke. Growing experimental evidence suggests that cerebral ischemia induces vascularization and angiogenesis (Wei et al., 2001). After stroke, vascularization and angiogenesis are necessary to sustain the supply of oxygen and nutrients to the brain. More importantly, endothelial cells produce signals for the reparative regeneration of the central nervous system by releasing angiocrine factors (Butler et al., 2010). An angiogenic niche may provide a novel interface where endothelial cells, perivascular cells, and circulating factors interact to control brain homeostasis by augmenting neurovascular remodeling after brain injury (Ohab et al., 2006; Butler et al., 2010). Along with enhanced angiogenesis, we observed a beneficial effect of post-stroke CIMT treatment on motor and cognitive function. The Morris water maze is a common experimental tool used to assess hippocampal-dependent spatial learning and memory function. Spatial learning appears to depend on a functionally integrated neural network. CIMT is considered an attractive restorative therapy because it enhances structural plasticity and functional reorganization. Our results suggest that CIMT may also promote hippocampal function. These results suggest that angiogenesis may be involved in repairing the brain after CIMT treatment of cerebral ischemia.

We found that, in ischemia/reperfusion rats, the ability to recover from functional deficits was deficient, possibly because a favorable environment for the proliferation and migration of new cells towards the infarct did not occur (Wiltout et al., 2007). Vascular endothelial cells and neighboring neurons are integrated within the neurovascular unit, and injury to any component of this unit may cause disorders of the system (Mabuchi et al., 2005). Most adult neural precursor proliferation occurs in an angiogenic environment, where neuronal, endothelial, and glial precursors differentiate in tight clusters. Exercise provides pleiotropic protective effects after stroke far more than angiogenesis alone. For example, Qu et al. (2015) demonstrated that forced limb-use was facilitative for neuronal proliferation after cerebral ischemia. Consistent with this finding, in the current study, a mild increase in newborn nestin- and DCX-positive cells was observed in the subventricular zone in ischemia/reperfusion rats, while CIMT had a strong effect on endogenous neurogenesis after stroke. However, it is known that although a substantial number of new precursors are produced and migrate out from the subventricular zone after cerebral ischemia, only a small number of them differentiate and survive in the long-term (Thored et al., 2006). Similar to the increased neurogenesis that was observed in the subventricular zone, there was an increase in newborn NeuN- and GFAP-positive cells in the ischemic boundary zone after CIMT. This suggests that the newborn microvessels that are induced by CIMT may promote the proliferation of endogenous nerve precursor cells in the subventricular zone, as well as their migration to the infarct area and their further differentiation into mature neurons and glial cells. The pro-

liferation, differentiation, and migration of newborn cells may thus be facilitated by CIMT.

In the present study, CIMT visibly increased the densities of  $\alpha$ -SMA<sup>+</sup> cells in the ischemic boundary zone compared with fasudil treatment. Endothelial cells play critical roles in initiating angiogenesis, and vascular smooth muscle cells contribute to vascular maturation and arteriogenesis (Heil et al., 2006). In the current study, overexpression of both CD31 and  $\alpha$ -SMA suggest that CIMT treatment contributes to both angiogenic initiation and vascular maturation. We demonstrated that CIMT treatment protected the neurovascular unit against decline, including a preservation of pericytes and a reduction in tight junction damage. Growing evidence indicates that pericytes are critical for blood-brain barrier maintenance, blood flow, and vessel stability (Winkler et al., 2011; Obermeier et al., 2013). Pericyte-endothelial cell interactions play a key role in regulating the formation of tight junctions and vesicle trafficking in endothelial cells, and blood-brain barrier dysfunction and neuroinflammation may be caused if these interactions are disrupted during central nervous system injury (Daneman et al., 2010). Blood-brain barrier properties are mainly determined by endothelial tight junctions. The expression of claudin-5, a tight junction protein, was visibly increased by CIMT. Our data suggest that CIMT may help to promote ischemic injury repair of the blood-brain barrier in the chronic post-stroke period, which is regulated by pericytes.

Our data demonstrate the positive impact of CIMT on post-stroke angiogenesis, neurogenesis, and blood-brain barrier integrity, but the mechanisms involved remain unknown. There was a significant reduction in the expression levels of Nogo-A/RhoA/ROCK in the peri-infarct cortex in CIMT-treated rats in this study, which is consistent with results from a previous study (Zhao et al., 2013). Nogo-A is a myelin-associated neurite growth inhibitor and is responsible for the limitation of the regenerative capacity in the central nervous system (GrandPré et al., 2000; Prinjha et al., 2000). Anti-Nogo-A immunotherapy may contribute to improvement in cognitive function and synaptic plasticity (Tews et al., 2013), and Nogo-A deactivation enhances neuroplasticity and functional recovery after stroke in adult rats (Taub et al., 2006; Tsai et al., 2007; Gillani et al., 2010). A recent report indicates that Nogo-A exerts its inhibitory effects on angiogenesis in the early postnatal brain through the intracellular activation of the RhoA/ROCK/Myosin II pathway (Wälchli et al., 2013). RhoA and its first effector, ROCK, have been reported to participate in the pathogenesis of atherosclerotic cardiovascular disease (Shimokawa et al., 2005). Furthermore, 14 weeks of exercise training downregulates RhoA gene expression in rat endothelial cells (Matsumoto et al., 2012). The ROCK inhibitor fasudil stimulates axonal regrowth, increases cerebral blood flow, and protects against neuronal cell death in rats after cerebral ischemia (Toshima et al., 2000; Rikitake et al., 2005; Yamashita et al., 2007). In our study, treatment with a neutralizing antibody against ROCK resulted in marked angiogenesis, neurogenesis, and functional recovery. More importantly, CIMT low-

ered RhoA and ROCK levels to the same extent as NEP1-40 at 4 weeks after MCAO. These results confirmed that CIMT promotes post-stroke angiogenesis and neurogenesis, at least in part, by overcoming Nogo-A/RhoA/ROCK signaling. However, in the early stages of ischemia/reperfusion (2 weeks after MCAO), CIMT treatment did not decrease the expression levels of Nogo-A/RhoA/ROCK as much as treatment with NEP1-40; this indicates that the positive effects of CIMT are time-dependent.

We also demonstrated that, compared with the fasudil group, angiogenesis, neurogenesis and functional recovery were markedly increased in the CIMT1 group at 4 weeks after MCAO. Further investigation revealed that CIMT increased VEGFR2-positive cell numbers in the ischemic boundary zone of the impaired cortex after stroke, whereas there was no change in VEGFR2-positive cell numbers in fasudil-treated rats compared with IR rats. Previous studies have reported that VEGFR2 is an important regulator of signal transduction in VEGF-A-mediated central nervous system angiogenesis (Mancuso et al., 2008). Our results suggest that other mechanisms, such as the VEGF-A/VEGFR2 pathway, may compensate for the influence of Nogo-A/RhoA/ROCK on CIMT-induced central nervous system neuroprotection.

The limitations of the present study include statistical limitations because of small sample size and insufficiency of randomization. In this study, a random method was adopted when the rats were initially grouped. However, because a small number of rats died during the experiment, rats were added at random to ensure sufficient numbers of rats in each group; this did not guarantee complete randomness. Based on the positive results, we will have a longer-term study in the future and supplement TUNEL staining.

In summary, CIMT promoted post-stroke regenerative repair at least in part by overcoming the Nogo-A/RhoA/ROCK signaling pathway in a time-dependent manner.

**Acknowledgments:** We thank Qianze Dong from Department of Pathology, College of Basic Medical Sciences of China Medical University, China and Guifeng Zhao from Experimental Research Center, Shengjing Hospital of China Medical University, China for excellent technical assistance.

**Author contributions:** Scientific and accurate analysis: JF; result analysis and discussion: ZYZ and JF; study design, principal investigator, manuscript drafting and revising: ZYZ. Both authors have read and approved the final manuscript.

**Conflicts of interest:** The authors declare that there are no conflicts of interest associated with this manuscript.

**Financial support:** This study was supported by the National Natural Science Foundation of China (General Program), No. 81771271 (to JF). The funding source had no role in study conception and design, data analysis or interpretation, paper writing or deciding to submit this paper for publication.

**Institutional review board statement:** All protocols were approved by the Institutional Animal Care and Use Committee of China Medical University, China on December 9, 2015 (approval No. 2015PS326K). All experimental procedures described here were in accordance with the National Institutes of Health (NIH) guidelines for the Care and Use of Laboratory Animals (Publication No. 85-23, revised 1996).

**Copyright license agreement:** The Copyright License Agreement has been signed by both authors before publication.

**Data sharing statement:** Datasets analyzed during the current study

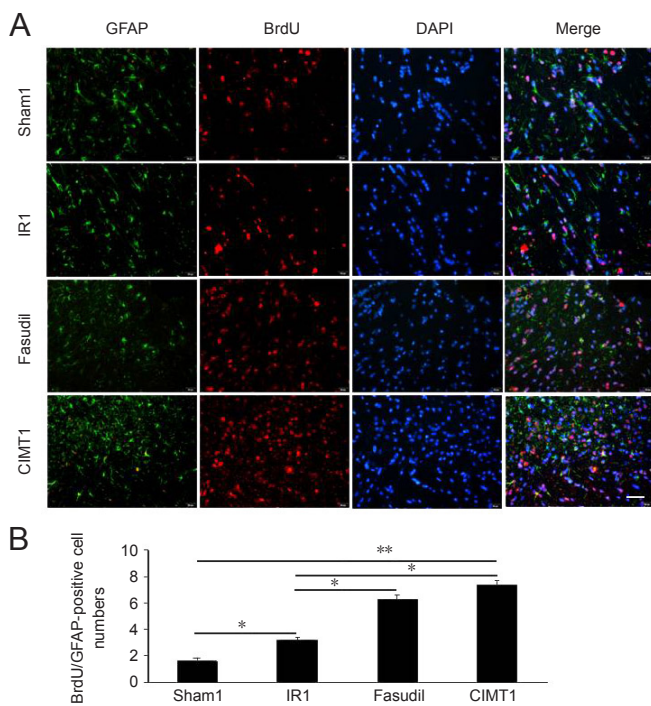


**Figure 7 CIMENT increases gliogenesis in the ischemic boundary zone.** (A) Double immunofluorescence images of BrdU/GFAP-positive cells in the Sham1 (no MCAO, vehicle), IR1 (MCAO + vehicle), fasudil (MCAO + a ROCK inhibitor fasudil), and CIMENT1 (MCAO + CIMENT) groups at 4 weeks after stroke. Nuclei were labeled blue by DAPI, GFAP-positive cells were labeled green by FITC, and BrdU-positive cells were labeled red by Cy3. Scale bar: 100  $\mu$ m. (B) Quantitative determination of mean BrdU/GFAP-positive cell numbers. BrdU/GFAP-positive cells were quantified by counting at a 400 $\times$  microscopic field of view. Data are expressed as the mean  $\pm$  SD ( $n = 5$ ; one-way analysis of variance followed by the Student-Newman-Keuls *post hoc* analysis). \* $P < 0.05$ , \*\* $P < 0.01$ . CIMENT: Constraint-induced movement therapy; IR: ischemia/reperfusion; DAPI: 4',6-diamidino-2-phenylindole.

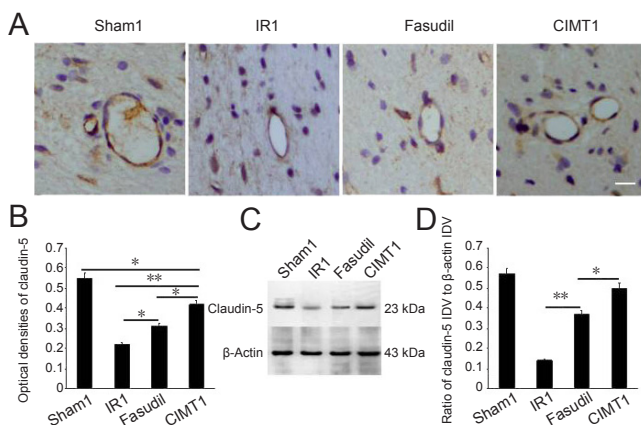


**Figure 8 Distribution and expression of claudin-5 in ischemic cerebral microvessels.** (A) Immunohistochemistry images of claudin-5 at 4 weeks after middle cerebral artery occlusion. Scale bar: 10  $\mu$ m. (B) Mean optical densities of claudin-5. (C) Representative protein expression bands of claudin-5 as measured by western blot assay at 4 weeks after middle cerebral artery occlusion. (D) The ratio of claudin-5 IDV to  $\beta$ -actin IDV 4 weeks after middle cerebral artery occlusion. (B, D) Data are expressed as the mean  $\pm$  SD ( $n = 5$ ; one-way analysis of variance followed by the Student-Newman-Keuls *post hoc* analysis). \* $P < 0.05$ , \*\* $P < 0.01$ . CIMENT: Constraint-induced movement therapy; IR: ischemia/reperfusion; IDV: integrated density value; MCAO: middle cerebral artery occlusion.

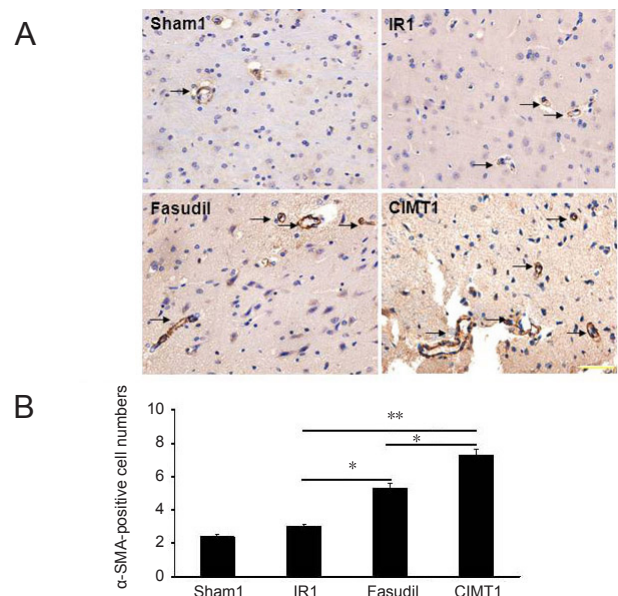


**Figure 9 Expression of the pericyte marker  $\alpha$ -SMA in the ischemic boundary zone at 4 weeks after middle cerebral artery occlusion.** (A) Immunohistochemistry images of  $\alpha$ -SMA. Black arrows indicate  $\alpha$ -SMA-positive cells. Scale bar: 50  $\mu$ m. (B) Quantitative determination of mean  $\alpha$ -SMA-positive cell numbers. The  $\alpha$ -SMA-positive cells were quantified by counting at a 400 $\times$  microscopic field of view. Data are expressed as the mean  $\pm$  SD ( $n = 5$ ; one-way analysis of variance followed by the Student-Newman-Keuls *post hoc* analysis). \* $P < 0.05$ , \*\* $P < 0.01$ . CIMENT: Constraint-induced movement therapy; IR: ischemia/reperfusion;  $\alpha$ -SMA:  $\alpha$ -smooth muscle actin; MCAO: middle cerebral artery occlusion. Sham1: No MCAO, vehicle; IR1: MCAO + vehicle; fasudil: MCAO + a ROCK inhibitor fasudil; CIMENT1: MCAO + CIMENT.

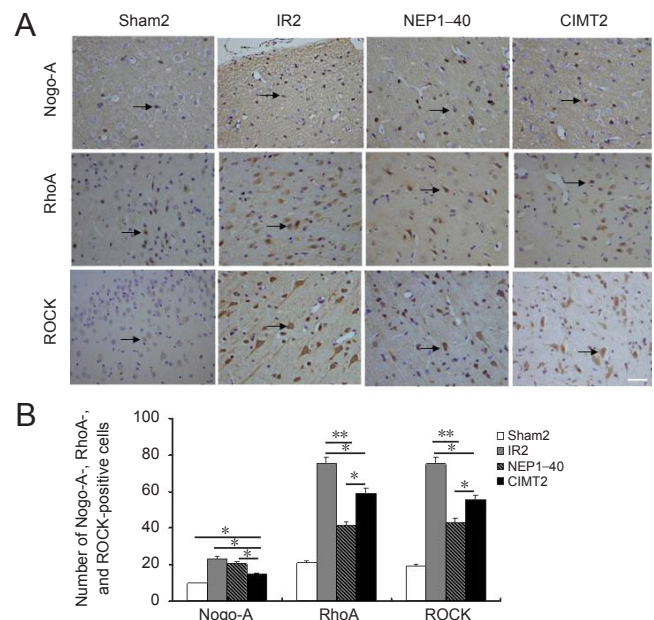


**Figure 10 Immunohistochemistry of Nogo-A, RhoA, and ROCK in the ischemic boundary zone at 2 weeks after middle cerebral artery occlusion.** (A) Immunohistochemistry images of Nogo-A, RhoA, and ROCK. Black arrows indicate Nogo-A-, RhoA-, or ROCK-positive cells. Scale bar: 50  $\mu$ m. (B) The mean numbers of Nogo-A, RhoA, and ROCK. Nogo-A-, RhoA-, or ROCK-positive cells were quantified by counting at a 400 $\times$  microscopic field of view. Data are expressed as the mean  $\pm$  SD ( $n = 5$ ; one-way analysis of variance followed by the Student-Newman-Keuls *post hoc* analysis). \* $P < 0.05$ , \*\* $P < 0.05$ . CIMENT: Constraint-induced movement therapy; IR: ischemia/reperfusion; ROCK: Rho-associated coiled-coil containing protein kinase. Sham2: No MCAO, vehicle; IR2: MCAO + vehicle; NEP1-40: MCAO + a specific antagonist of the Nogo-66 receptor NEP1-40; CIMENT2: MCAO + CIMENT.

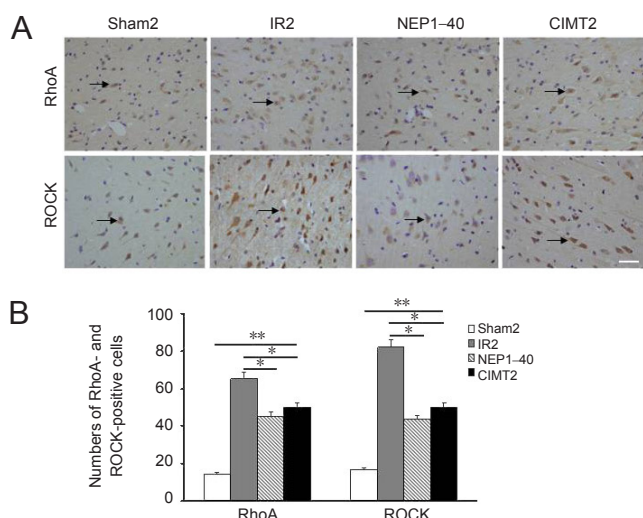


**Figure 11 Immunohistochemistry showing the protein expression levels of RhoA and ROCK in the ischemic boundary zone at 4 weeks after middle cerebral artery occlusion.** (A) Immunohistochemistry images of RhoA and ROCK. Black arrows indicate RhoA- or ROCK-positive cells. Scale bar: 50  $\mu$ m. (B) Quantification data of mean numbers of RhoA and ROCK. RhoA- and ROCK-positive cells were quantified by counting at a 400 $\times$  microscopic field of view. Data are expressed as the mean  $\pm$  SD ( $n = 5$ ; one-way analysis of variance followed by the Student-Newman-Keuls *post hoc* analysis). \* $P < 0.05$ , \*\* $P < 0.01$ . CIMT: Constraint-induced movement therapy; IR: ischemia/reperfusion; ROCK: Rho-associated coiled-coil containing protein kinase. Sham2: No MCAO, vehicle; IR2: MCAO + vehicle; NEP1-40: MCAO + a specific antagonist of the Nogo-66 receptor NEP1-40; CIMT2: MCAO + CIMT.

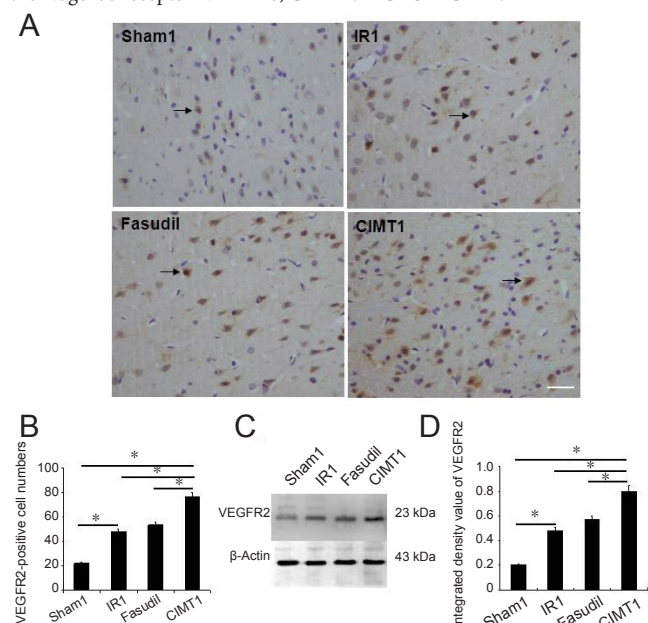


**Figure 12 Increased expression of VEGFR2 in the ischemic boundary zone after CIMT.** (A) Immunohistochemistry images of VEGFR2-positive cells in the ischemic boundary zone of the impaired cortex at 4 weeks after middle cerebral artery occlusion. Black arrows indicate VEGFR2-positive cells. Scale bar: 50  $\mu$ m. (B) Quantitative determination of mean VEGFR2-positive cell numbers. VEGFR2-positive cells were quantified by counting at a 400 $\times$  microscopic field of view. (C) Representative protein expression bands of VEGFR2 as measured by western blot assay. (D) Quantitative determination showed that CIMT treatment significantly increased VEGFR2 expression in cerebral ischemic rats. (B, D) Data are expressed as the mean  $\pm$  SD ( $n = 5$ ; one-way analysis of variance followed by the Student-Newman-Keuls *post hoc* analysis). \* $P < 0.05$ . CIMT: Constraint-induced movement therapy; IR: ischemia/reperfusion; VEGFR2: vascular endothelial growth factor receptor 2. Sham1: No MCAO, vehicle; IR1: MCAO + vehicle; fasudil: MCAO + a ROCK inhibitor fasudil; CIMT1: MCAO + CIMT.

are available from the corresponding author on reasonable request.

**Plagiarism check:** Checked twice by iThenticate.

**Peer review:** Externally peer reviewed.

**Open access statement:** This is an open access journal, and articles are distributed under the terms of the Creative Commons Attribution-Non-Commercial-ShareAlike 4.0 License, which allows others to remix, tweak, and build upon the work non-commercially, as long as appropriate credit is given and the new creations are licensed under the identical terms.

**Open peer reviewers:** Noela Rodriguez-Losada, Department of Human Physiology, University of Malaga and Biomedicine Biomedical Research Institute of Malaga (IBIMA), Spain; Elizabeth J. Sandquist, Weber State University, USA.

**Additional file:** Open peer review report 1 and 2.

## References

- Bregman BS, Kunkel-Bagden E, Schnell L, Dai HN, Gao D, Schwab ME (1995) Recovery from spinal cord injury mediated by antibodies to neurite growth inhibitors. *Nature* 378:498-501.
- Butler JM, Kobayashi H, Rafii S (2010) Instructive role of the vascular niche in promoting tumour growth and tissue repair by angiocrine factors. *Nat Rev Cancer* 10:138-146.
- Cao Y, Dong YX, Xu J, Chu GL, Yang ZH, Liu YM (2016) Spatiotemporal expression of Nogo-66 receptor after focal cerebral ischemia. *Neural Regen Res* 11:132-136.
- Chen MS, Huber AB, van der Haar ME, Frank M, Schnell L, Spillmann AA, Christ F, Schwab ME (2000) Nogo-A is a myelin-associated neurite outgrowth inhibitor and an antigen for monoclonal antibody IN-1. *Nature* 403:434-439.
- Daneman R, Zhou L, Kebede AA, Barres BA (2010) Pericytes are required for blood-brain barrier integrity during embryogenesis. *Nature* 468:562-566.
- Faulkner J, Wright A (2018) Using robotic-assisted technology to improve lower-limb function in people with stroke. *Clin Trials Degener Dis* 3:111-114.
- Gertz K, Priller J, Kronenberg G, Fink KB, Winter B, Schröck H, Ji S, Milosevic M, Harms C, Böhm M, Dirnagl U, Laufs U, Endres M (2006) Physical activity improves long-term stroke outcome via endothelial nitric oxide synthase-dependent augmentation of neovascularization and cerebral blood flow. *Circ Res* 99:1132-1140.
- Gillani RL, Tsai SY, Wallace DG, O'Brien TE, Arhebamen E, Tole M, Schwab ME, Kartje GL (2010) Cognitive recovery in the aged rat after stroke and anti-Nogo-A immunotherapy. *Behav Brain Res* 208:415-424.
- Ginsberg MD (2008) Neuroprotection for ischemic stroke: past, present and future. *Neuropharmacology* 55:363-389.
- Gonzenbach RR, Schwab ME. Disinhibition of neurite growth to repair the injured adult CNS: focusing on Nogo (2008) *Cell Mol Life Sci* 65:161-176.
- GrandPré T, Nakamura F, Vartanian T, Strittmatter SM (2000) Identification of the Nogo inhibitor of axon regeneration as a Reticulon protein. *Nature* 403:439-444.
- Heil M, Eitenmüller I, Schmitz-Rixen T, Schaper W (2006) Arteriogenesis versus angiogenesis: similarities and differences. *J Cell Mol Med* 10:45-55.
- Hermann DM, Chopp M (2012) Promoting brain remodeling and plasticity for stroke recovery: therapeutic promise and potential pitfalls of clinical translation. *Lancet Neurol* 11:369-380.
- Hill J, Rom S, Ramirez SH, Persidsky Y (2014) Emerging roles of pericytes in the regulation of the neurovascular unit in health and disease. *J Neuroimmune Pharmacol* 9:591-605.
- Hosseini-Sharifabad A, Mohammadi-Eraghi S, Tabrizian K, Soodi M, Khorshid Ahmad T, Naghdi N, Abdollahi M, Beyer C, Roghani A, Sharifzadeh M (2011) Effects of training in the Morris water maze on the spatial learning acquisition and VAcHT expression in male rats. *Daru* 19:166-172.
- Huber AB, Weinmann O, Brösamle C, Oertle T, Schwab ME (2002) Patterns of Nogo mRNA and protein expression in the developing and adult rat and after CNS lesions. *J Neurosci* 22:3553-3567.
- Hunter AJ, Hatcher J, Virley D, Nelson P, Irving E, Hadingham SJ, Parsons AA (2000) Functional assessments in mice and rats after focal stroke. *Neuropharmacology* 39:806-816.

- Intracerebral hemorrhage after intravenous t-PA therapy for ischemic stroke (1997) The NINDS t-PA Stroke Study Group. *Stroke* 28:2109-2118.
- Ishida A, Misumi S, Ueda Y, Shimizu Y, Cha-Gyun J, Tamakoshi K, Ishida K, Hida H (2015) Early constraint-induced movement therapy promotes functional recovery and neuronal plasticity in a subcortical hemorrhage model rat. *Behav Brain Res* 284:158-166.
- Kartje GL, Schulz MK, Lopez-Yunez A, Schnell L, Schwab ME (1999) Corticostriatal plasticity is restricted by myelin-associated neurite growth inhibitors in the adult rat. *Ann Neurol* 45:778-786.
- Lee JK, Kim JE, Sivula M, Strittmatter SM (2004) Nogo receptor antagonism promotes stroke recovery by enhancing axonal plasticity. *J Neurosci* 24:6209-6217.
- Lei C, Wu B, Cao T, Liu M, Hao Z (2016) Brain recovery mediated by toll-like receptor 4 in rats after intracerebral hemorrhage. *Brain Res* 1632:1-8.
- Liebscher T, Schnell L, Schnell D, Scholl J, Schneider R, Gullo M, Fouad K, Mir A, Rausch M, Kindler D, Hamers FP, Schwab ME (2005) Nogo-A antibody improves regeneration and locomotion of spinal cord-injured rats. *Ann Neurol* 58:706-719.
- Longa EZ, Weinstein PR, Carlson S, Cummins R (1989) Reversible middle cerebral artery occlusion without craniectomy in rats. *Stroke* 20:84-91.
- Lu Y, Hsiang F, Chang JH, Yao XQ, Zhao H, Zou HY, Wang L, Zhang QX (2018) Houshiheisan and its components promote axon regeneration after ischemic brain injury. *Neural Regen Res* 13:1195-1203.
- Mabuchi T, Lucero J, Feng A, Koziol JA, del Zoppo GJ (2005) Focal cerebral ischemia preferentially affects neurons distant from their neighboring microvessels. *J Cereb Blood Flow Metab* 25:257-266.
- Madri JA (2009) Modeling the neurovascular niche: implications for recovery from CNS injury. *J Physiol Pharmacol* 60:95-104.
- Mancuso MR, Kuhnert F, Kuo CJ (2008) Developmental angiogenesis of the central nervous system. *Lymphat Res Biol* 6:173-180.
- Marsh SA, Coombes JS (2005) Exercise and the endothelial cell. *Int J Cardiol* 99:165-169.
- Matsumoto A, Mason SR, Flatscher-Bader T, Ward LC, Marsh SA, Wilce PA, Fasset RG, de Haan JB, Coombes JS (2012) Effects of exercise and antioxidant supplementation on endothelial gene expression. *Int J Cardiol* 158:59-65.
- Obermeier B, Daneman R, Ransohoff RM (2013) Development, maintenance and disruption of the blood-brain barrier. *Nat Med* 19:1584-1596.
- Ohab JJ, Fleming S, Blesch A, Carmichael ST (2006) A neurovascular niche for neurogenesis after stroke. *J Neurosci* 26:13007-13016.
- Palmer TD, Willhoite AR, Gage FH (2000) Vascular niche for adult hippocampal neurogenesis. *J Comp Neurol* 425:479-494.
- Paxinos G, Watson C (2005) The rat brain in stereotaxic coordinates. 5<sup>th</sup> ed. Oxford: Elsevier Academic Press.
- Peng ZM, Zhao XY, Zhu K, Wan Y (2018) Lingo-1 regulates neural stem cell differentiation via Rho-ROCK signaling pathway. *Zhongguo Zuzhi Gongcheng Yanjiu* 22:4669-4674.
- Prinjha R, Moore SE, Vinson M, Blake S, Morrow R, Christie G, Michalovich D, Simmons DL, Walsh FS (2000) Inhibitor of neurite outgrowth in humans. *Nature* 403:383-384.
- Qu HL, Zhao M, Zhao SS, Xiao T, Song CG, Cao YP, Jolkkonen J, Zhao CS (2015) Force limb-use enhanced neurogenesis and behavioral recovery after stroke in the aged rats. *Neuroscience* 286:316-324.
- Quaeghebeur A, Lange C, Carmeliet P (2011) The neurovascular link in health and disease: molecular mechanisms and therapeutic implications. *Neuron* 71:406-424.
- Rikitake Y, Kim HH, Huang Z, Seto M, Yano K, Asano T, Moskowitz MA, Liao JK (2005) Inhibition of Rho kinase (ROCK) leads to increased cerebral blood flow and stroke protection. *Stroke* 36:2251-2257.
- Ruan L, Wang B, ZhuGe Q, Jin K (2015) Coupling of neurogenesis and angiogenesis after ischemic stroke. *Brain Res* 1623:166-173.
- Saver JL, Gornbein J, Grotta J, Liebeskind D, Lutsep H, Schwamm L, Scott P, Starkman (2009) Number needed to treat to benefit and to harm for intravenous tissue plasminogen activator therapy in the 3- to 4.5-hour window: joint outcome table analysis of the ECASS 3 trial. *Stroke* 40:2433-2437.
- Schnell L, Schwab ME (1990) Axonal regeneration in the rat spinal cord produced by an antibody against myelin-associated neurite growth inhibitors. *Nature* 343:269-272.
- Shen Q, Goderie SK, Jin L, Karanth N, Sun Y, Abramova N, Vincent P, Pumiglia K, Temple S (2004) Endothelial cells stimulate self-renewal and expand neurogenesis of neural stem cells. *Science* 304:1338-1340.
- Shimokawa H, Takeshita A (2005) Rho-kinase is an important therapeutic target in cardiovascular medicine. *Arterioscler Thromb Vasc Biol* 25:1767-1775.
- Sterling C, Taub E, Davis D, Rickards T, Gauthier LV, Griffin A, Uswatte G (2013) Structural neuroplastic change after constraint-induced movement therapy in children with cerebral palsy. *Pediatrics* 131:e1664-1669.
- Taguchi A, Soma T, Tanaka H, Kanda T, Nishimura H, Yoshikawa H, Tsukamoto Y, Iso H, Fujimori Y, Stern DM, Naritomi H, Matsuyama T (2004) Administration of CD34<sup>+</sup> cells after stroke enhances neurogenesis via angiogenesis in a mouse model. *J Clin Invest* 114:330-338.
- Taub E, Uswatte G (2006) Constraint-induced movement therapy: answers and questions after two decades of research. *NeuroRehabilitation* 21:93-95.
- Tews B, Schöning K, Arzt ME, Clementi S, Rioult-Pedotti MS, Zemar A, Berger SM, Schneider M, Enkel T, Weinmann O, Kasper H, Schwab ME, Bartsch D (2013) Synthetic microRNA-mediated downregulation of Nogo-A in transgenic rats reveals its role as regulator of synaptic plasticity and cognitive function. *Proc Natl Acad Sci U S A* 110:6583-6588.
- Thored P, Arvidsson A, Cacci E, Ahlenius H, Kallur T, Darsalia V, Ekdahl CT, Kokaia Z, Lindvall O (2006) Persistent production of neurons from adult brain stem cells during recovery after stroke. *Stem Cells* 24:739-747.
- Toshima Y, Satoh S, Ikegaki I, Asano T (2000) A new model of cerebral microthrombosis in rats and the neuroprotective effect of a Rho-kinase inhibitor. *Stroke* 31:2245-2250.
- Tsai SY, Markus TM, Andrews EM, Cheatwood JL, Emerick AJ, Mir AK, Schwab ME, Kartje GL (2007) Intrathecal treatment with anti-Nogo-A antibody improves functional recovery in adult rats after stroke. *Exp Brain Res* 182:261-266.
- Tsai SY, Papadopoulos CM, Schwab ME, Kartje CL (2011) Delayed anti-nogo-a therapy improves function after chronic stroke in adult rats. *Stroke* 42:186-190.
- Ueno Y, Choppe M, Zhang L, Buller B, Liu Z, Lehman NL, Liu XS, Zhang Y, Roberts C, Zhang ZG (2012) Axonal outgrowth and dendritic plasticity in the cortical peri-infarct area after experimental stroke. *Stroke* 43:2221-2228.
- Wälchli T, Pernet V, Weinmann O, Shiu JY, Guzik-Kornacka A, Decrey G, Yüksel D, Schneider H, Vogel J, Ingber DE, Vogel V, Frei K, Schwab ME (2013) Nogo-A is a negative regulator of CNS angiogenesis. *Proc Natl Acad Sci U S A* 110:E1943-1952.
- Wei L, Erinjeri JP, Rovainen CM, Woolsey TA (2001) Collateral growth and angiogenesis around cortical stroke. *Stroke* 32:2179-2184.
- Wiltout C, Lang B, Yan Y, Dempsey RJ, Vemuganti R (2007) Repairing brain after stroke: a review on post-ischemic neurogenesis. *Neurochem Int* 50:1028-1041.
- Winkler EA, Bell RD, Zlokovic BV (2011) Central nervous system pericytes in health and disease. *Nat Neurosci* 14:1398-1405.
- Yamashita K, Kotani Y, Nakajima Y, Shimazawa M, Yoshimura S, Nakashima S, Iwama T, Hara H (2007) Fasudil, a Rho kinase (ROCK) inhibitor, protects against ischemic neuronal damage in vitro and in vivo by acting directly on neurons. *Brain Res* 1154:215-224.
- Zhao CS, Puurunen K, Schallert T, Sivenius J, Jolkkonen J (2005) Effect of cholinergic medication, before and after focal photothrombotic ischemic cortical injury, on histological and functional outcome in aged and young adult rats. *Behav Brain Res* 156:85-94.
- Zhao S, Zhao M, Xiao T, Jolkkonen J, Zhao C (2013) Constraint-induced movement therapy overcomes the intrinsic axonal growth-inhibitory signals in stroke rats. *Stroke* 44:1698-1705.

P-Reviewers: Rodriguez-Losada N, Sandquist EJ; C-Editor: Zhao M; S-Editors: Wang J, Li CH; L-Editors: Gardner B, Stow A, Qiu Y, Song LP; T-Editor: Liu XL